Investigating the subendocardial dark rim artefact in first-pass myocardial perfusion

P. F. Ferreira[1], P. D. Gatehouse[2], and D. N. Firmin[2]
[1]Royal Brompton Hospital, London, London, United Kingdom, [2]Royal Brompton Hospital, London, United Kingdom

Aim
The purpose of this work was to compare the dark-rim artifact in myocardial perfusion sequences using flexible phantom models of the LV myocardium and blood, with realistic MRI and susceptibility properties.

Introduction
First-pass myocardial perfusion imaging with Gd-DTPA contrast agent (CA) is entering clinical use with generally promising performance. However, subendocardial dark rim artifacts (DRA) resembling perfusion defects are frequently reported. The DRA is typically discriminated from a stress-induced defect by: 1) comparing stress versus rest perfusion injections, but this can be deceptive due to residual CA, changes in wall motion and CA bolus due to stress, or 2) the short persistence of DRA and its correlation with the left ventricle (LV) blood brightness, but this decreases sensitivity to mild stress-induced defects. Several reasons for DRA have been demonstrated: motion of the heart walls [8], Gibbs-artifact [1], Mz-recovery during imaging-time [4] and susceptibility [6]. These are difficult to study in-vivo due to residual CA and limitations on the total CA dose. In this study the myocardium and the LV were modeled using gelatin to assess the DRA with perfusion sequences.

Methods
The first-pass peak was modelled estimating 0.5% of Gd-DTPA (Omniscan; Nycomed Amersham, Amersham UK) (100%=0.5mol/L) in the myocardium and 0 to 2% in the LV blood [2, 3]. Myocardial T1=79ms, T2=34ms and blood T1=42/21ms, and T2=34/18ms, at 1%/2% CA respectively. Susceptibility was modelled taking into consideration that 6% CA approximately cancels water diamagnetism, and the diamagnetism of oxygenated blood without CA is similar to water [5, 7]. The diamagnetism of the undiluted gelatin used was also found to be similar to water. A hollow cylinder of undiluted gelatin (T1=70ms, T2=26ms) (height=9.5cm, inner radius=4cm, outer radius=7.5cm) was used to simulate the myocardial wall. The inside was filled with 0 to 2% CA in distilled water to simulate the LV blood pool. A time-series of T1-weighted images showed negligible dissolving of the gelatin within 30 minutes, which allowed these models to be used for MR perfusion studies. The cylinder axis was oriented at a range of angles, α, to B0 as in the varying cardiac orientations between patients, as it is well known that geometry alters B0 distortion. Perfusion images were acquired following clinical established protocols (h-EPI: TR=7.6ms, TE=1.32ms, 2.8 x 2.8 x 8 mm, flip angle=30°, time delay from saturation to the centre of k-space (TD) of 80 ms, EPI factor of 4; FLASH: TR=1.5ms, TE=1.17ms, 2.8 x 2.8 x 8 mm, flip angle=12°, TD of 80 ms; b-SSFP: TR=1.9ms, TE=1.13ms, 2.8 x 2.8 x 8 mm, flip angle=50°,TD of 80 ms). The three sequences had TSENSE incorporated with an acceleration factor of 2. To further identify artifact sources, images were repeated with phase-encode direction flipped, and with saturation off, in order to obtain the same signal for the gelatin and the Gd-DTPA solution suppressing any possible Gibbs artifact. Field plots were also acquired to visualise the field distortions.

Results and Discussion

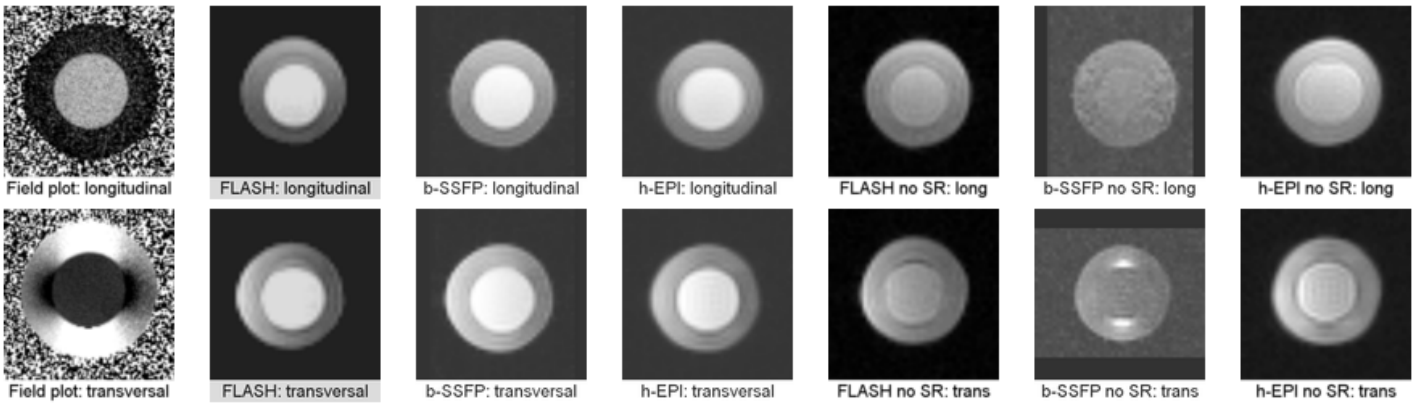

Figure 1: Field plots and FLASH/b-SSFP/h-EPI TSENSE images at 2% Gd in longitudinal (above) and transversal (bottom) orientations in relation to the main field. On the three right-most columns the sequences were implemented with the Saturation recovery turned off. The gradient of brightness is due to the use of a surface coil.

Field plots show that as the angle α increases, field distortions increase in the gelatin (except in the diagonal directions) while keeping the field constant in the Gd-solution (Left of Figure 1). Using no saturation preparation, coupled with low flip angles, the difference between signals in the subendocardium border was negligible, nulling Gibbs-artifact, with the three sequences showing an increase in the DRA as α increased, suggesting that some of the artifact's extent has susceptibility as its nature. The diagonal parts are not affected by the DRA, in this case, which sustains the susceptibility hypothesis (three right-most columns of Figure 1).
With saturation on, DRA are more pronounced as α increased for the h-EPI sequence, while it is fairly constant in FLASH and b-SSFP, without any motion (2^{nd} to 4^{th} columns of Figure 1). This shows that while in the h-EPI sequence, susceptibility seems to be the leading cause of artifact, for the FLASH and b-SSFP sequences we have Gibbs-artifacts as the main cause, in the absence of motion.
Work in progress includes motion, compressing and expanding the model rapidly during imaging to model cardiac function; it also includes modelling different stages of the first-pass by altering the CA concentration in the model.

Conclusion
The dark rim artifact is visible all around the myocardium and it seems to be a mixture of Gibbs and susceptibility artifacts. Comparing the same image with and without a saturation preparation for the h-EPI sequence, suggests that some of its extent is due to susceptibility. Comparing the three sequences we can also infer that h-EPI is more prone to DRA than FLASH or b-SSFP, especially when the heart is in the transverse orientation in relation to the main field.

References
[1] E Di Bella, et al., MRM, 54(5):1295. [2] A Elkington, et al., JMRI, 21(4):354. [3] F Epstein, et al., MRM, 47(3):482. [4] J Hennig, et al., MRM, 48(5):801. [5] R Mulkern, et al., MRI, 23(6):757. [6] W Schreiber, et al., JMRI, 16(6):641. [7] W Spees, et al., MRM, 45(4):533. [8] P Storey, et al., MRM, 48(6):1028.